Vapor−Liquid Phase Boundaries of Binary Mixtures of Carbon Dioxide with Ethanol and Acetone

Hung-Yu Chiu, Ming-Jer Lee,* and Ho-mu Lin

Department of Chemical Engineering, National Taiwan University of Science and Technology, 43 Keelung Road, Section 4, Taipei 106-07, Taiwan

A visual and volume-variable high-pressure phase equilibrium analyzer (PEA) was used for measuring the isothermal vapor−liquid equilibrium (VLE) phase boundaries of CO_2 + ethanol and CO_2 + acetone at temperatures from (291.15 to 313.15) K over a wide composition range. The isothermal phase equilibrium properties obtained from this work were compared with literature values to clarify the inconsistency of the VLE data taken from different sources. The new VLE data were correlated with the Soave−Redlich−Kwong, the Peng−Robinson, and the Patel−Teja equations of state incorporating with the one-parameter and the two-parameter van der Waals one-fluid mixing rules, respectively.

Introduction

The phase behavior of the mixtures containing supercritical fluid (SCF) at elevated pressures has received particular attention in the last few decades. The phase equilibrium properties of the related mixtures are essentially needed in the development of supercritical fluid techniques for SCF extraction,[1] reaction,[2] fractionation,[3] nanoparticle formation,[4−7] etc. Carbon dioxide has been recognized as an environmentally benign solvents and widely used in the SCF applications because it has mild critical conditions (T_c = 304.25 K, P_c = 7.38 MPa) and is inexpensive, nontoxic, nonflammable, and readily available. Ethanol and acetone are commonly used organic solvents in chemical, petroleum, and polymer industries. In the SCF applications, these two substances are often served as cosolvents in extraction processes to enhance the solubility of polar constituents in the SCF-rich phase and also used as solvents in the supercritical antisolvent (SAS) process to generate Ultrafine particles for a variety of materials.[4−7] Recently, several investigators[6−11] pointed out that the phase behavior of solvent + antisolvent mixtures is one of the crucial factors to govern the morphology and the mean size of the resultant particles produced from the SAS process. In general, nanometric particles, micrometric particles, and dense films could be obtained when the SAS precipitation was conducted in supercritical, superheated vapor, and vapor−liquid coexistence phase regions,[11] respectively. As a consequence, the VLE phase diagram of solvent + antisolvent systems is fundamentally important for manipulating precipitation conditions to prepare particulate products with preferable dimension and morphology. The VLE phase boundaries near the critical region are especially of interest in developing the SCF micronization processes. Table 1 listed the selected VLE data sources[12−32] for CO_2 + ethanol and CO_2 + acetone. Figures 1 and 2 show that those available data of CO_2 + ethanol and CO_2 + acetone are not well-consistent, particularly at temperatures lower than 313 K. In the present study, a visual and volume-variable phase equilibrium analyzer (PEA) was utilized to observe the phase transition boundaries of mixture samples changing from the single phase into the vapor−liquid coexistence region. Since the operation of the PEA is based on a synthetic method, it is especially applicable to determine the phase boundaries near the critical region, in which the analytic method often fails. The isothermal VLE phase boundaries were measured for the binary systems composed of CO_2 with ethanol and acetone at temperatures from (298.15 to 313.15) K over a

Table 1. VLE Data Sources for CO_2 + Ethanol and CO_2 + Acetone Systems

T/K	P/MPa	authors	reference
	CO_2 + ethanol		
291.15 to 313.14	0.91 to 7.92	Day et al.	12
291.15 to 323.15	3.3 to 8.11	Stievano and Elvassore	13
333.2 to 496	6.74 to 14.91	Wu et al.	14
318.15	8.6 to 8.8	Wang et al.	15
313.4 to 344.75	0.57 to 11.93	Perakis et al.	16
313.2 to 328.2	1.6 to 9.42	Tsivintzelis et al.	17
313.2 to 353.2	1.31 to 13.9	Kneza et al.	18
323.15	5.03 to 8.2	Chen et al.	19
298.15 to 413.15	6.181 to 15.147	Yeo et al.	20
313.2	0.6 to 7.55	Yoon et al.	21
313.14 to 333.4	0.514 to 10.654	Suzuki and Sue	22
313.4 to 344.75	0.59 to 11.97	Joung et al.	23
312.82 to 373	0.476 to 14.345	Galicia-Luna and Ortega-Rodriguez	24
373.15	7.0 to 15.0	Pfohl et al.	25
314.5 to 337.2	5.55 to 10.845	Jennings et al.	26
298.15	1.55 to 5.9	Kordikowski et al.	27
	CO_2 + acetone		
291.15 to 313.13	0.78 to 7.39	Day et al.	12
291.15 to 323.15	0.7 to 4.02	Stievano and Elvassore	13
333.2 to 482	6.74 to 11.79	Wu et al.	14
308.6 to 332.2	7.78 to 9.58	Reaves et al.	28
303 to 332.9	1.05 to 8.1	Bamberger and Maurer	29
298.15 to 313.15	0.395 to 7.411	Katayama et al.	30
313.15 to 333.15	0.987 to 9.603	Adrian and Maurer	31
298.15	2.153 to 3.368	Kato et al.	32

Table 2. Properties of Pure Compounds[a]

compound	MW/g·mol^{-1}	T_c/K	P_c/MPa	ω
carbon dioxide	44.01	304.1	7.38	0.225
ethanol	46.07	513.9	6.14	0.644
acetone	58.08	508.1	4.70	0.304

[a] Reid et al.[36]

* Corresponding author. E-mail: mjlee@mail.ntust.edu.tw. Tel.: +886-2-2737-6626. Fax: +886-2-2737-6644.

10.1021/je800371a CCC: $40.75
Published on Web 08/27/2008

Table 3. VLE Phase Boundaries of Carbon Dioxide + Ethanol

	P/MPa				
CO_2 mole fraction	291.15 K	298.17 K	303.12 K	308.11 K	313.14 K
0.192	2.45	2.79	2.99	3.27	3.51
0.289	3.14	3.82	4.08	4.52	4.86
0.364	3.81	4.37	4.77	5.17	5.61
0.488	4.59	5.05	5.63	6.16	6.68
0.587	5.02	5.49	6.01	6.62	7.18
0.706	5.18	5.75	6.33	6.9	7.58
0.800	5.30	5.90	6.48	7.08	7.78
0.834	5.35	5.95	6.53	7.13	7.83
0.860	5.40	5.97	6.57	7.18	7.88
0.893	5.43	5.98	6.62	7.19	7.96
0.924	5.45	6.08	6.67	7.30	8.05
0.954	5.49	6.22	6.81	7.44	8.18
0.985	5.53	6.37	7.04	7.69	7.80[a]

[a] Dew point.

Table 4. VLE Phase Boundaries of Carbon Dioxide + Acetone

	P/MPa				
CO_2 mole fraction	291.15 K	298.16 K	303.13 K	308.15 K	313.15 K
0.198	0.72	0.83	0.95	1.09	1.22
0.297	1.21	1.46	1.59	1.76	1.97
0.396	1.78	2.02	2.22	2.47	2.75
0.498	2.39	2.71	2.98	3.30	3.53
0.597	3.02	3.44	3.75	4.14	4.47
0.699	3.59	4.05	4.43	4.88	5.34
0.802	4.26	4.80	5.21	5.58	6.18
0.831	4.40	4.94	5.46	5.92	6.51
0.862	4.61	5.16	5.68	6.25	6.80
0.892	4.85	5.45	5.99	6.48	7.18
0.922	5.06	5.70	6.28	6.85	7.43
0.953	5.34	6.02	6.57	7.23	7.88
0.984	5.52	6.43	7.05	7.73	7.95[a]

[a] Dew point.

Table 5. Estimated Critical Conditions for Binary Systems of Carbon Dioxide (1) with Ethanol (2) or Acetone (2)

compd (2)	*T*/K	P_c/MPa	x_{1c}
ethanol	313.14	8.18	0.955
	313.2[a]	8.15[a]	0.97[a]
acetone	313.15	8.01	0.973
	313.25[b]	8.048[b]	0.973[b]

[a] Yoon et al.[21] [b] Ardian and Maurer.[31]

wide composition range, including near critical regions. These new binary VLE data were compared with literature values taken from various sources. The experimental VLE data were also correlated with the Soave−Redlich−Kwong (SRK),[33] the Peng−Robinson (PR),[34] and the Patel−Teja (PT)[35] equations of state (EOS) incorporating with the van der Waals (vdW) one-fluid mixing rules, respectively.

Experimental Section

Materials. Carbon dioxide (purity of 99.5+ %) was purchased from Liu-Hsiang Co. (Taiwan), acetone, halocarbons free grade (99.9 %), from Arcos (USA), and ethanol, HPLC grade (99.99 %), from Fisher Scientific (USA). All the chemicals were used without further purification. The physical properties of these compounds are listed in Table 2.

Apparatus. The schematic diagram and operation procedure of the visual and volume-variable PEA have been given in detail elsewhere.[37] This apparatus consists of a high-pressure generator (model 62-6-10, High Pressure Equipment Co., USA) equipped with a sapphire window (Part No. 742.0106, Bridgman closure, SITEC, Switzerland), a rupture disk, and a circulation jacket. The visualized cell is operable up to 50 MPa and 473.15 K. The cell's temperature was controlled by circulated thermostatic water and measured by an inserted thermocouple, whose reading has been calibrated to within an uncertainty of 0.1 K. A pressure transducer (PDCR 407-01, Druck, UK) with a digital display (DPI 280, Druck, UK) measured the cell's pressure to within an uncertainty of 0.04 %. Each component was charged individually into the cell by a precision syringe pump (model: 260D, Isco Inc., USA). The weight of each loaded substance was calculated from the known charged volume and its density at charging pressure and temperature. The charged volumes were read from the control panel of the syringe pumps which are accurate to 0.01 cm^3. While the densities of carbon dioxide were taken from the NIST Chemistry WebBook,[38] the densities of the pure organic liquids were determined experimentally in our research laboratory by a high-pressure densitometer (DMA 512P, Anton Paar, Austria) with an oscillation period indicator (DMA 48, Anton Paar, Austria) to an uncertainty of 0.0001 $g \cdot cm^{-3}$. The uncertainty of the composition of the loaded mixtures was estimated to be 0.003 in mole fraction. The phase behavior of the mixture in the cell was observed with the aid of a digital camera, LED-white light, and a television. The loaded sample was compressed to form a single phase at a fixed temperature, and pressure was then slowly decreased until the second phase appeared by manipulating manually the position of the piston in the high-pressure generator. The uncertainty of the observed phase transition pressures was estimated to be 0.02 MPa. In our previous paper,[37] the VLE data of CO_2 + 1-octanol have been measured and compared with the data

Table 6. Calculated Results for Carbon Dioxide (1) + Ethanol (2)

EOS	MR	k_{ij}	l_{ij}	$(\Delta x_1/x_1)$ % AAD
		$T = 291.15$ K		
SRK	Q1	0.0980		8.6
	Q2	0.1072	0.0305	5.1
PR	Q1	0.1049		9.7
	Q2	0.1250	0.0514	9.6
PT	Q1	0.0888		10.0
	Q2	0.1057	0.0559	8.6
		$T = 298.16$ K		
SRK	Q1	0.0962		8.2
	Q2	0.0958	0.0200	7.6
PR	Q1	0.1049		10.3
	Q2	0.1053	0.0302	9.5
PT	Q1	0.0883		9.6
	Q2	0.0874	0.0381	9.2
		$T = 303.13$ K		
SRK	Q1	0.0884		9.4
	Q2	0.0934	0.0155	8.8
PR	Q1	0.1028		10.1
	Q2	0.1020	0.0207	9.7
PT	Q1	0.0852		9.7
	Q2	0.0852	0.0160	9.1
		$T = 308.15$ K		
SRK	Q1	0.0899		7.5
	Q2	0.0888	0.0002	6.9
PR	Q1	0.1060		12.0
	Q2	0.0961	0.0083	8.4
PT	Q1	0.0891		12.3
	Q2	0.0791	0.0092	8.2
		$T = 313.13$ K		
SRK	Q1	0.0891		7.8
	Q2	0.0884	0.0002	7.5
PR	Q1	0.0944		8.4
	Q2	0.0944	0.0067	8.0
PT	Q1	0.0776		8.1
	Q2	0.0770	0.0061	8.0

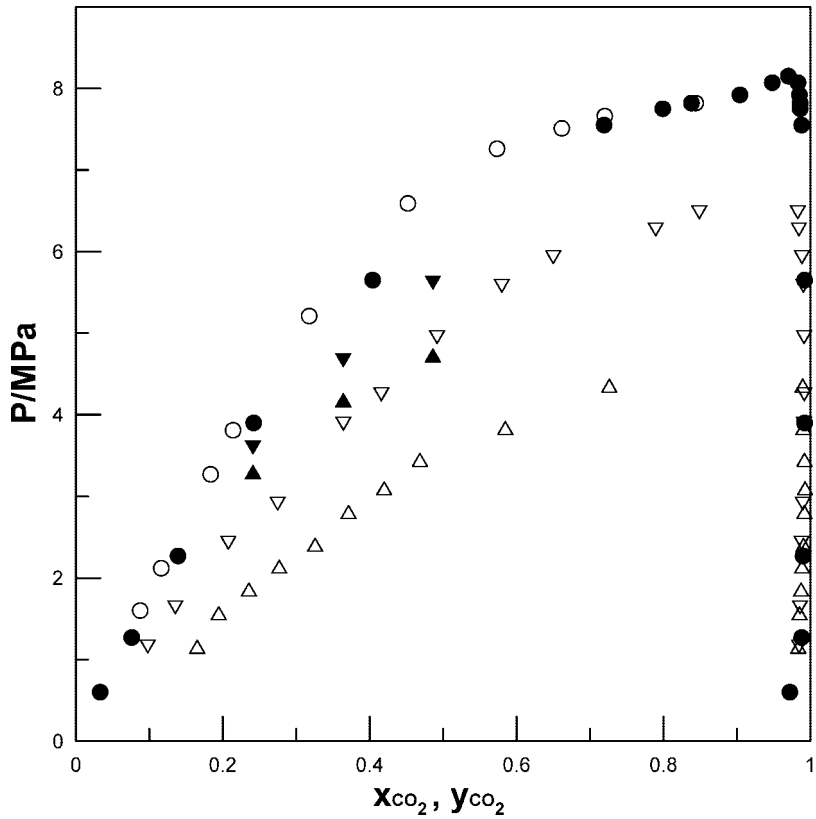

Figure 1. Comparison of VLE literature data for CO_2 (1) + ethanol (2): Δ, 291.15 K, Day et al.;[12] ▲, 291.15 K, Stievano and Ekvassore;[13] ∇, 303.12 K, Day et al.;[12] ▼, 303.15 K, Stievano and Ekvassore;[13] ○, 313.2 K, Tsivintzelis et al.;[17] ●, 313.2 K, Yoon et al.[21]

taken from a semiflow-type VLE apparatus. The determined bubble pressures agreed with the literature values to within 2.7 %.

Results and Discussion

In the present study, the PEA apparatus was used to measure the isothermal VLE phase boundaries for two CO_2-containing systems in a temperature range of (291.15 to 313.15) K. Tables 3 and 4 report the determined phase boundary data for CO_2 + ethanol and CO_2 + acetone, respectively. Over the entire experimental conditions, the majority of data points are bubble points, and only one dew point was observed at 313.15 K from each binary system. Figures 3 and 4 present, respectively, these isothermal VLE phase boundaries varying with mole fraction of carbon dioxide, indicating that the solubility of carbon dioxide in ethanol or acetone increases with increasing pressure and decreases with temperature. The right end of the isotherms of (291 to 303) K (below the critical temperature of carbon dioxide) should correspond to the vapor pressures of carbon dioxide, while each supercritical isotherm [(308 or 313) K] should exhibit a maximum pressure, i.e., mixture's critical point, at a certain composition of carbon dioxide. As shown in Figures 3 and 4 and the tabulated values, the critical composition at 308 K should be greater than 0.984, in the mole fraction of carbon dioxide, for each binary system. Meanwhile, the critical pressure and critical composition at 313 K can be estimated from the maximum pressure point of the isothermal VLE phase boundary by interpolation. Table 5 lists the estimated critical pressure and the critical mole fraction of carbon dioxide at 313 K for these two investigated binary systems. As also seen from Table 5, the critical pressures determined from this study are in good agreement

Table 7. Calculated Results for Carbon Dioxide (1) + Acetone (2)

EOS	MR	k_{ij}	l_{ij}	$(\Delta x_1/x_1)$ % AAD
		T = 291.15 K		
SRK	Q1	0.0082		5.6
	Q2	0.066	0.0985	1.9
PR	Q1	0.0084		5.8
	Q2	0.0652	0.0874	1.2
PT	Q1	0.009		6.1
	Q2	0.0704	0.1188	2.2
		T = 298.16 K		
SRK	Q1	−0.0005		3.2
	Q2	0.0277	0.0521	1.6
PR	Q1	0.0045		3.6
	Q2	0.0361	0.0507	1.3
PT	Q1	0.0012		3.5
	Q2	0.0326	0.0666	1.4
		T = 303.13 K		
SRK	Q1	−0.002		2.6
	Q2	0.0190	0.0395	1.1
PR	Q1	0.0034		2.9
	Q2	0.0281	0.0404	1.0
PT	Q1	−0.0009		3.2
	Q2	0.0229	0.0513	1.1
		T = 308.15 K		
SRK	Q1	−0.0028		2.0
	Q2	0.0062	0.0181	1.4
PR	Q1	0.0055		2.4
	Q2	0.0196	0.0241	1.3
PT	Q1	−0.0023		2.5
	Q2	0.0135	0.0260	1.4
		T = 313.13 K		
SRK	Q1	0.0031		6.3
	Q2	0.0393	0.0029	6.3
PR	Q1	0.0264		4.4
	Q2	0.0334	0.0114	3.7
PT	Q1	−0.0241		4.8
	Q2	0.0332	0.0180	4.0

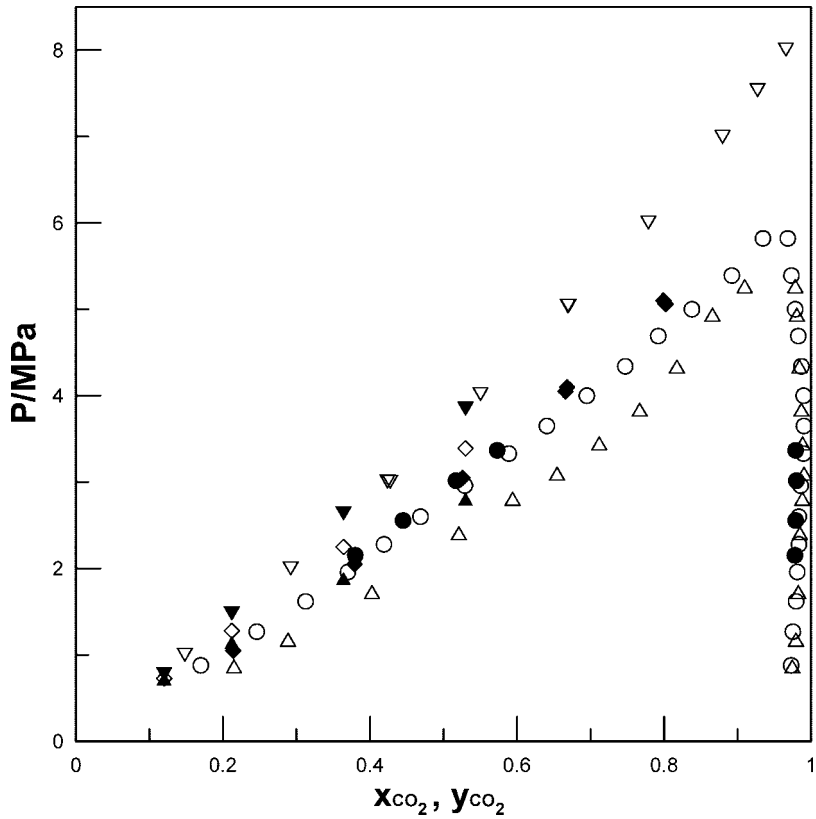

Figure 2. Comparison of VLE literature data for CO_2 (1) + acetone (2): Δ, 291.15 K, Day et al.;[12] ▲, 291.15 K, Stievano and Elvassore;[13] ○, 298.15 K, Day et al.;[12] ●, 298.15 K, Kato et al.;[32] ◇, 303.15 K, Stievano and Elvassore;[13] ◆, 303.15 K, Bamberger and Maurer;[29] ∇, 313.15 K, Adrian and Maurer;[31] ▼, 313.15 K, Stievano and Elvassore.[13]

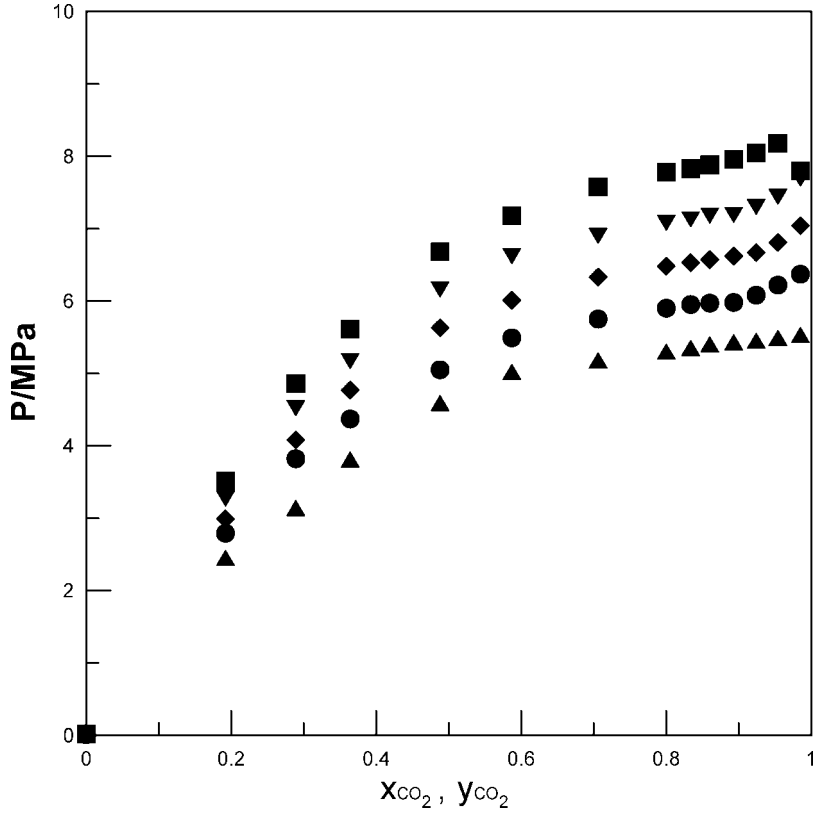

Figure 3. VLE phase boundaries for CO_2 (1) + ethanol (2): ▲, 291.15 K; ●, 298.17 K; ◆, 303.12 K; ▼, 308.11 K; ■, 313.14 K.

with the literature values for both CO_2 + ethanol[21] and CO_2 + acetone,[31] and the deviations are within 0.038 MPa.

As mentioned earlier, one of the main objectives of this study is to clarify the inconsistent VLE data reported by different investigators for CO_2 + ethanol and CO_2 + acetone. Figures 5, 6, and 7 compare the phase boundaries of the CO_2 + ethanol system obtained from different sources at 291 K/313 K, 298 K/308 K, and 303 K, respectively. It appears that our results

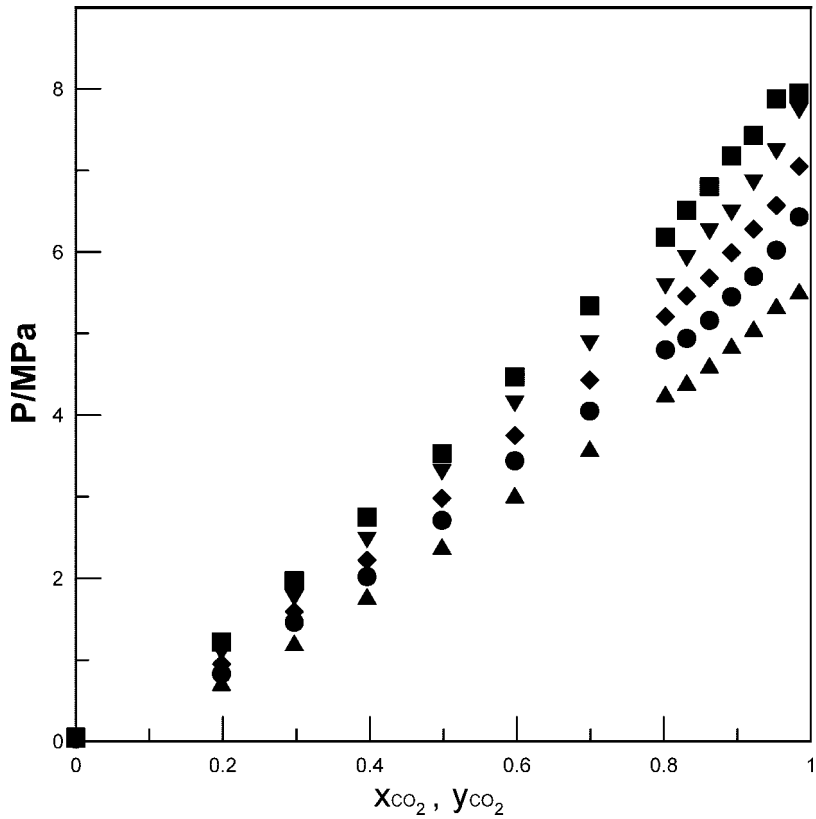

Figure 4. VLE phase boundaries for CO_2 (1) + acetone (2): ▲, 291.15 K; ●, 298.16 K; ◆, 303.13 K; ▼, 308.15 K; ■, 313.15 K.

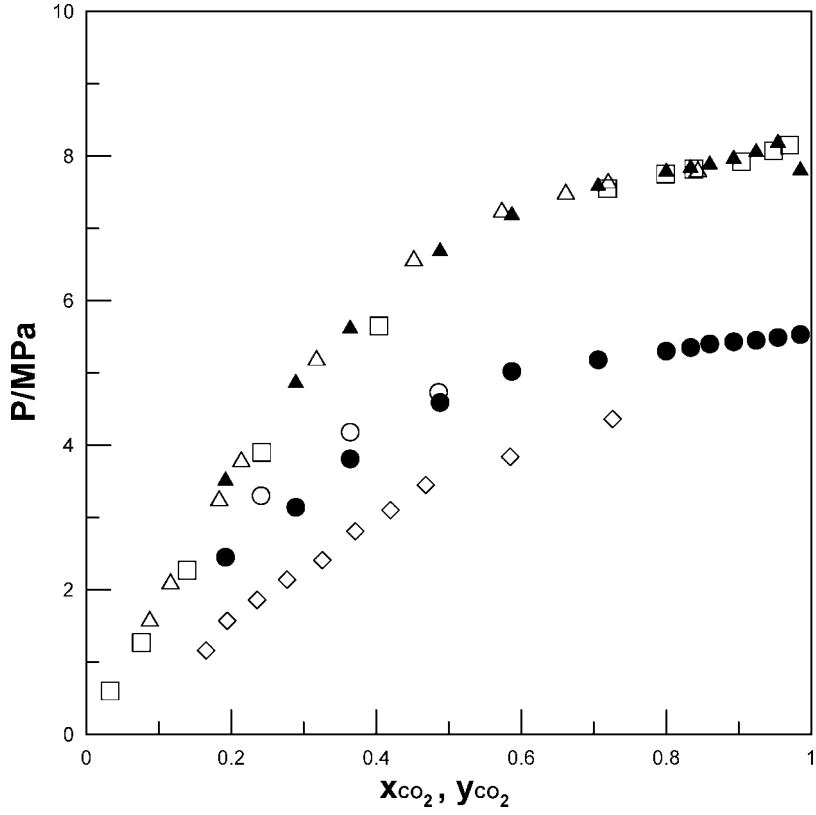

Figure 5. Comparison of the experimental results of this work with literature values for CO_2 (1) + ethanol (2) at (291 and 313) K: ●, 291.15 K; ▲, 313.14 K, this work; ○, 291.15 K, Stievano and Elvassore;[13] Δ, 313.2 K, Tsivintzelis et al.;[17] ◇, 291.15 K, Day et al.;[12] □, 313.2 K, Yoon et al.[21]

are consistent with those of Kordikowski et al.[27] (2.1 % AARD) at 298 K, Stievano and Elvassore[13] (1.2 % AARD) at 303 K, and Tsivintzelis et al.[17] (1.0 % AARD) and Yoon et al.[21] (3.2 % AARD) at 313 K but slightly lower than the data of Stievano and Elvassore[13] (6.4 % AARD) at 291 K. The bubble pressures at 291 K (21.1 % AARD), 303 K (11.9 % AARD), and 308 K (7.1 % AARD) reported by Day et al.[12] are relatively low, particularly in the region of lower CO_2 concentrations.

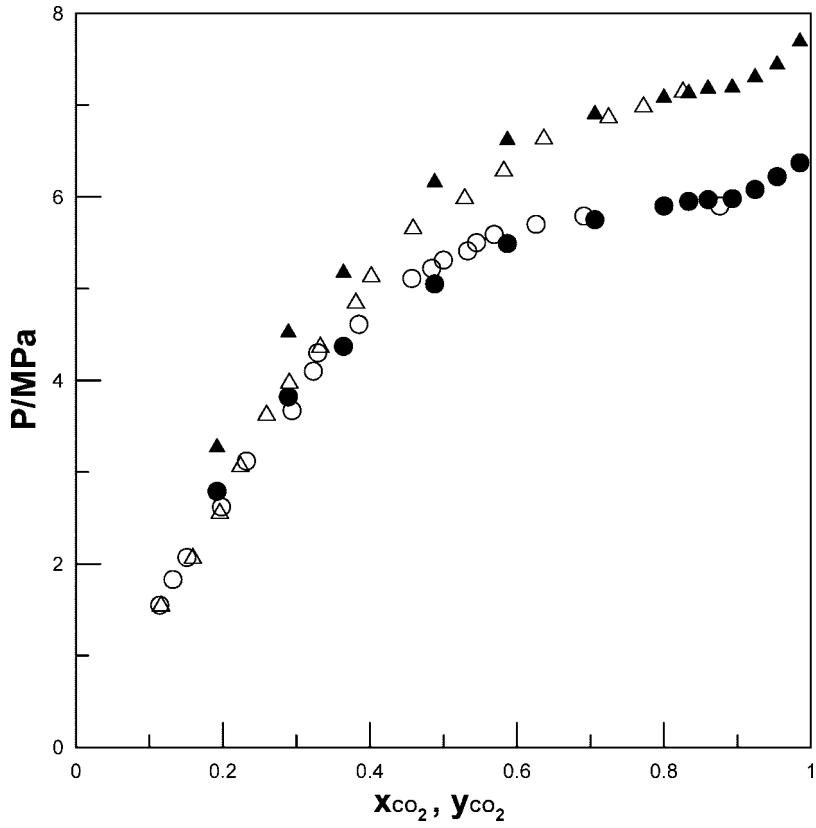

Figure 6. Comparison of the experimental results of this work with literature values for CO_2 (1) + ethanol (2) at (298 and 308) K: ●, 298.17 K; ▲, 308.11 K, this work; ○, 298.15 K, Kordikowski et al.;[27] Δ, 308.11 K, Day et al.[12]

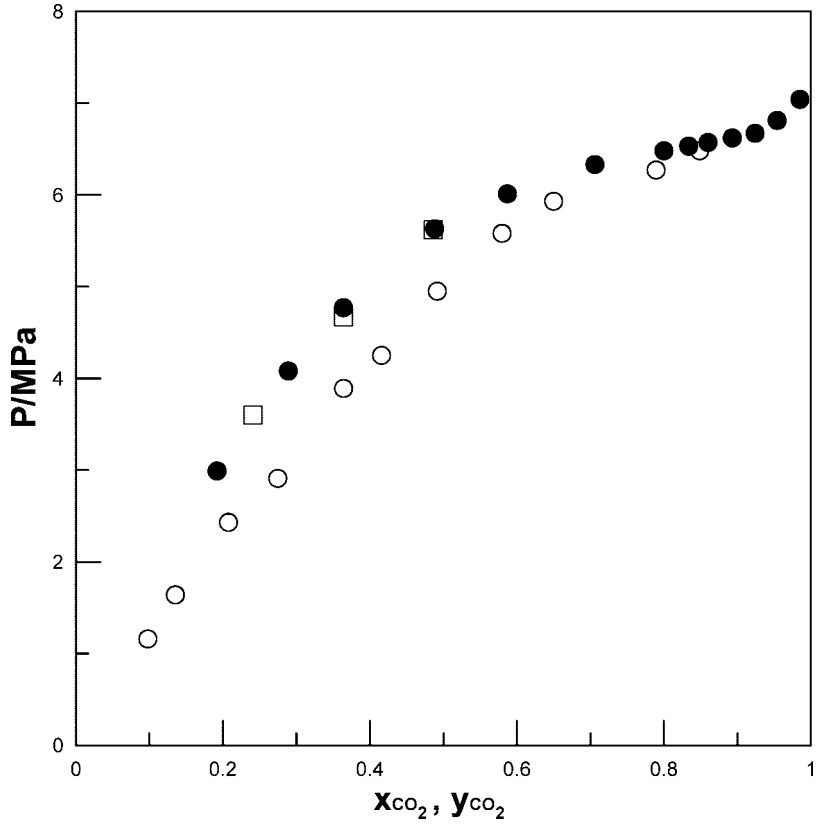

Figure 7. Comparison of the experimental results of this work with literature values for CO_2 (1) + ethanol (2) at 303 K: ●, 303.12 K, this work; ○, 303.12 K, Day et al.;[12] □, 303.15 K, Stievano and Elvassore.[13]

Figures 8 and 9 compare the phase boundaries of CO_2 + acetone at 291 K/303 K and 298 K/313 K, respectively. Our results agree well with those of Day et al.[12] at 291 K (4.2 % AARD) and 298 K (3.0 % AARD), Kato et al.[32] (1.9 % AARD) at 298 K, Bamberger and Maurer[29] at 303 K (3.7 % AARD), Ardian and Maurer[31] (1.9 % AARD) and Stievano and Elvas-

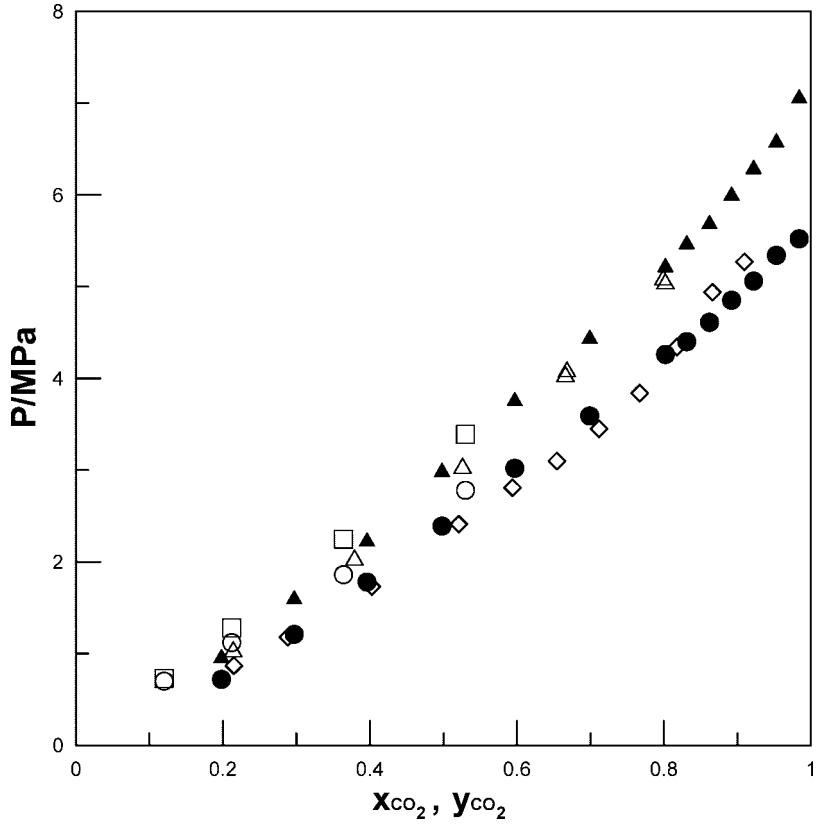

Figure 8. Comparison of the experimental results of this work with literature values for CO_2 (1) + acetone (2) at (291 and 308) K: ●, 291.15 K; ▲, 303.13 K, this work; ○, 291.15 K, Stievano and Elvassore;[13] Δ, 303 K, Bamberger and Maurer;[29] ◇, 291.15 K, Day et al.;[12] □, 303.15 K, Stievano and Elvassore.[13]

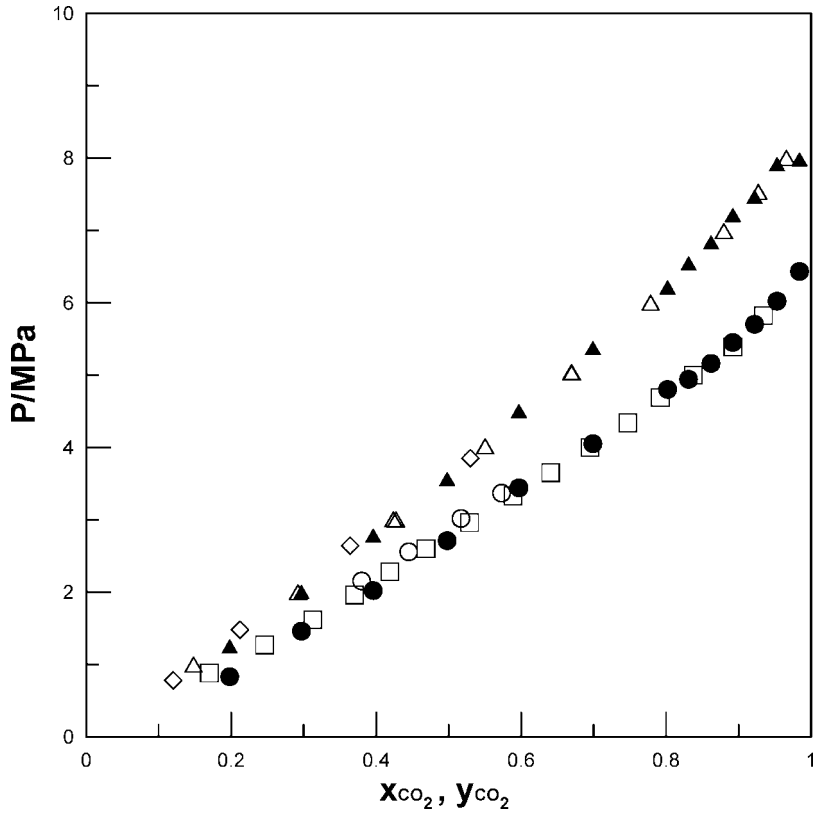

Figure 9. Comparison of the experimental results of this work with literature values for CO_2 (1) + acetone (2) at 303 K: ●, 298.16 K; ▲, 313.15 K, this work; ○, 298.15 K, Kato et al.;[32] Δ, 313.15 K, Ardian and Maurer;[31] □, 298.16 K, Day et al.;[12] ◇, 313.15 K, Stievano and Elvassore.[13]

sore[13] (6.9 % AARD) at 313 K. However, the bubble pressures reported by Stievano and Elvassore[13] at 291.15 K (15.8 % AARD) and 303.15 K (10.2 % AARD) are obviously higher than those measured by other investigators.

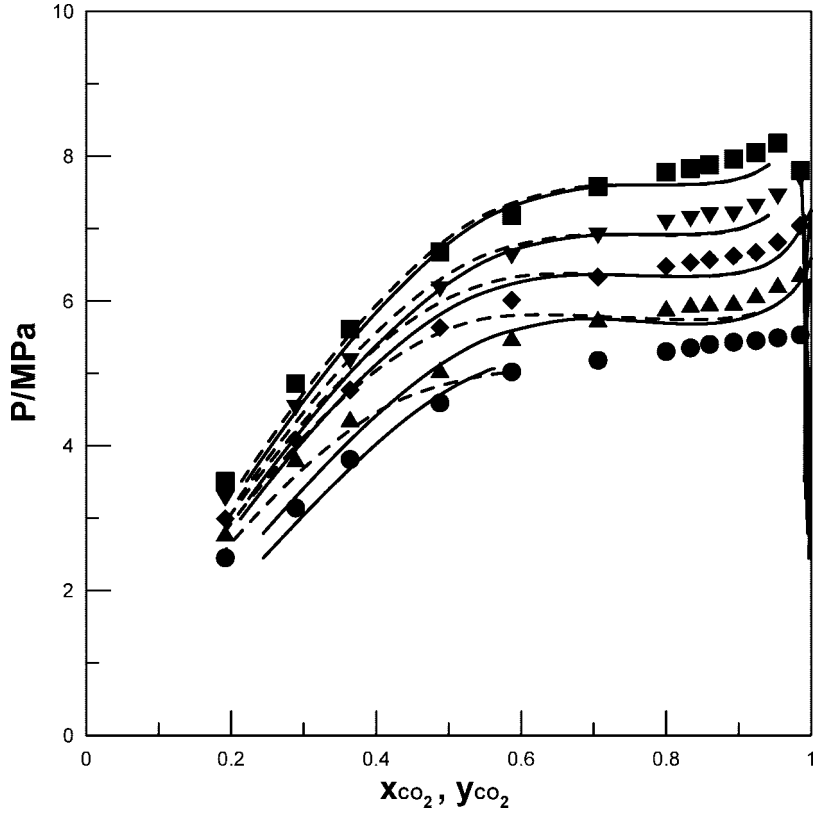

Figure 10. Comparison of the calculated results from the PR EOS with the experimental values for CO_2 (1) + ethanol (2): ●, 291.15 K; ▲, 298.17 K; ◆, 303.12 K; ▼, 308.11 K; ■, 313.14 K; ---, calcd, MR-Q1; —, calcd, MR-Q2.

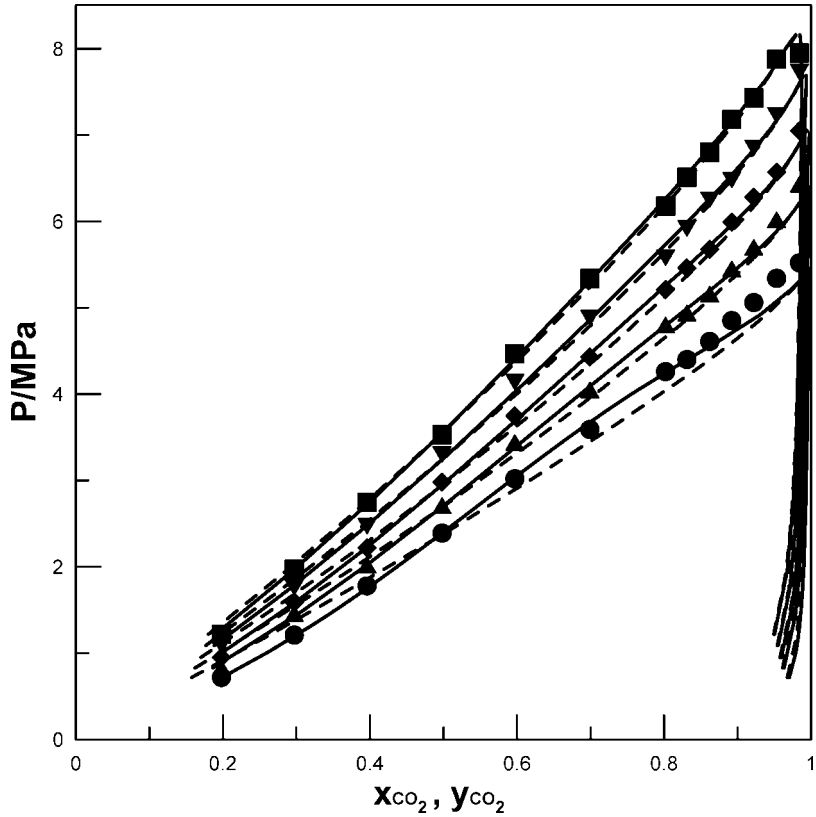

Figure 11. Comparison of the calculated results from the PR EOS with the experimental values for CO_2 (1) + acetone (2): ●, 291.15 K; ▲, 298.16 K; ◆, 303.13 K; ▼, 308.15 K; ■, 313.15 K; ---, calcd, MR-Q1; —, calcd, MR-Q2.

VLE Data Correlation. The VLE data were correlated with the Soave−Redlich−Kwong (SRK),[33] the Peng−Robinson (PR),[34] and the Patel−Teja (PT)[35] equations of state with the one-parameter vdW one-fluid mixing rule (MR-Q1) and the two-

parameter vdW one-fluid mixing rule (MR-Q2), respectively. The vdW one-fluid mixing rules for equation constants a_m, b_m, and c_m (c_m for the PT EOS only) were defined as

$$a_m = \sum_{i=1}^{n_c}\sum_{j=1}^{n_c} x_i x_j a_{ij} \quad (1)$$

$$b_m = \sum_{i=1}^{n_c}\sum_{j=1}^{n_c} x_i x_j b_{ij} \quad (2)$$

$$c_m = \sum_{i=1}^{n_c}\sum_{j=1}^{n_c} x_i x_j c_{ij} \quad (3)$$

with

$$a_{ij} = (1 - k_{ij})\sqrt{a_i a_j} \quad (4)$$

$$b_{ij} = (1 - l_{ij})(b_i + b_j)/2 \quad (5)$$

$$c_{ij} = (c_i + c_j)/2 \quad (6)$$

where n_c is the number of components and the subscripts of m, i, j, and ij represent the parameters for mixture, component i, component j, and $i-j$ pair interactions, respectively. The variables k_{ij} and l_{ij} are the binary interaction parameters. In the mixing rule of MR-Q1, the value of l_{ij} was set to zero. The optimal values of the binary interaction parameters at a given temperature were obtained from the isothermal flash calculation[39] by minimization of the following objective function π

$$\pi = \sqrt{\frac{1}{n}\sum_{k=1}^{n}\left[\left(\frac{x_{1,k}^{\mathrm{calcd}} - x_{1,k}^{\mathrm{exptl}}}{x_{1,k}^{\mathrm{exptl}}}\right)^2\right]} \quad (7)$$

where n is the number of experimental data points and the superscripts of calcd and exptl refer to the calculated and the experimental values, respectively. The calculation results for CO_2 + ethanol and CO_2 + acetone are compiled in Tables 6 and 7, respectively, where the entry of $(\Delta x_1/x_1)$ % AAD was defined as

$$(\Delta x_1/x_1)\ \%\ \mathrm{AAD} = \frac{100\ \%}{n}\sum_{k=1}^{n}\left|\frac{x_{1,k}^{\mathrm{calcd}} - x_{1,k}^{\mathrm{exptl}}}{x_{1,k}^{\mathrm{exptl}}}\right| \quad (8)$$

By using the same model (EOS together with the mixing rules), better results were obtained for CO_2 + acetone than those for CO_2 + ethanol. The tabulated values also reveal that the mixing rule is a more influential factor on the calculated deviations than the EOS. Only the calculated results from the Peng−Robinson EOS are thus presented in the following graphical comparisons. Figures 10 and 11 illustrate that the MR-Q2 yields better results, especially at temperatures lower than 304 K, regardless of the EOS used. In this lower temperature range, the MR-Q1 obviously underestimates the liquid composition, x_{CO2}. It should be also noted that the flash calculation failed to converge in the carbon dioxide-rich region at 291 K where the equations of state indicate that liquid−liquid phase splitting may occur, while the convergent problem did not encounter in CO_2 + acetone.

Conclusions

The vapor−liquid phase transition boundaries have been measured with a synthetic method for CO_2 + ethanol and CO_2 + acetone at temperatures from (291 to 313) K over a wide composition range. As evidenced from the experimental results, the solubilities of carbon dioxide in both ethanol and acetone increase with increasing pressure and decreasing temperature. Moreover, carbon dioxide is more soluble in acetone than in ethanol at the same conditions. The critical conditions at 313 K have also been determined in the present study by interpolation of the isothermal VLE phase boundary data for each binary system. Most importantly, the experimental results of this work are helpful in clarifying the inconsistency of literature VLE data taken from different sources for CO_2 + ethanol and CO_2 + acetone. The VLE data were correlated with the Soave−Redlich−Kwong, the Peng−Robinson, and the Patel−Teja equations of state incorporating with the one-parameter and the two-parameter van der Waals one-fluid mixing rules. The applicability of these three cubic equations of state is quite similar when the same mixing rule was adopted. In general, the use of the two-parameter vdW one-fluid mixing rule yielded satisfactory results for CO_2 + acetone, but a slight improvement was obtained for CO_2 + ethanol.

Acknowledgment

Thanks go to Professor Brunner's research group at the Technical University of Hamburg-Hamburg, Germany, for providing the phase equilibrium calculation package: PE 2000.

Literature Cited

(1) McHugh, M. A.; Krukonis, V. J. *Supercritical Fluid Extraction: Principles and Practice*, 2nd ed.; Butterworth Heinemann: Stoneham, MA, 1994.
(2) Nishi, K.; Morikawa, Y.; Misumi, R.; Kaminoyama, M. Radical Polymerization in Supercritical Carbon Dioxide−Use of Supercritical Carbon Dioxide as a Mixing Assistant. *Chem. Eng. Sci.* **2005**, *60*, 2419–2426.
(3) Eckert, C. A.; Ekart, M. P.; Knutson, B. L.; Payne, K. P.; Tomasko, D. L.; Liotta, C. L.; Foster, N. R. Supercritical Fluid Fractionation of a Nonionic Surfactant. *Ind. Eng. Chem. Res.* **1992**, *31*, 1105–1110.
(4) Reverchon, E. Supercritical Antisolvent Precipitation of Micro- and Nano-Particles. *J. Supercrit. Fluids* **1999**, *15*, 1–21.
(5) Jung, J.; Perrut, M. Particle Design Using Supercritical Fluids: Literature and Patent Survey. *J. Supercrit. Fluids* **2001**, *20*, 179–219.
(6) Wu, H. T.; Lee, M. J.; Lin, H. M. Nano-Particles Formation for Pigment Red 177 via a Continuous Supercritical Anti-solvent Process. *J. Supercrit. Fluids* **2005**, *33*, 173–182.
(7) Wu, H. T.; Lee, M. J.; Lin, H. M. Precipitation Kinetics of Pigment Blue 15:6 Sub-Micro Particles with a Supercritical Anti-Solvent Process. *J. Supercrit. Fluids* **2006**, *37*, 220–228.
(8) Wu, H. T.; Lin, H. M.; Lee, M. J. Ultra-Fine Particles Formation of C.I. Pigment Green 36 in Different Phase Regions via a Supercritical Anti-Solvent Process. *Dyes Pigments* **2007**, *75*, 328–334.
(9) Reverchon, E.; Caputo, G.; De Marco, I. Role of Phase Behavior and Atomization in the Supercritical Antisolvent Precipitation. *Ind. Eng. Chem. Res.* **2003**, *42*, 6406–6414.
(10) Reverchon, E. Micro and Nano Particles Produced by Supercritical Fluids Assisted Techniques: Present Status and Future Developments. *Chem. Eng. Trans.* **2002**, *2*, 1–10.
(11) Chang, S. C.; Lee, M. J.; Lin, H. M. The Influence of Phase Behavior on the Morphology of Protein α-Chymotrypsin Prepared via a Supercritical Anti-Solvent Process. *J. Supercrit. Fluids* **2008**, *44*, 219–229.
(12) Day, C. Y.; Chang, C. J.; Chen, C. Y. Phase Equilibrium of Ethanol + CO_2 and Acetone + CO_2 at Elevated Pressures. *J. Chem. Eng. Data* **1996**, *41*, 839–843.
(13) Stievano, M.; Elvassore, N. High-Pressure Density and Vapor-Liquid Equilibrium for the Binary Systems Carbon Dioxide-Ethanol, Carbon Dioxide-Acetone and Carbon Dioxide-Dichloromethane. *J. Supercrit. Fluids* **2005**, *33*, 7–14.
(14) Wu, W.; Ke, J.; Poliakoff, M. Phase Boundaries of CO_2 + Toluene, CO_2 + Acetone, and CO_2 + Ethanol at High Temperatures and High Pressures. *J. Chem. Eng. Data* **2006**, *51*, 1398–1403.
(15) Wang, B.; Han, B.; Jiang, T.; Zhang, Z.; Xie, Y.; Li, W.; Wu, W. Enhancing the Rate of the Diels-Alder Reaction Using CO_2 + Ethanol and CO_2 + *n*-Hexane Mixed Solvents of Different Phase Regions. *J. Phys. Chem. B* **2005**, *109*, 24203–24210.
(16) Perakis, C.; Voutsas, E.; Magoulas, K.; Tassios, D. Thermodynamic Modeling of the Vapor-Liquid Equilibrium of the Water/Ethanol/CO_2 System. *Fluid Phase Equilib.* **2006**, *243*, 142–150.

(17) Tsivintzelis, I.; Missopolinou, D.; Kalogiannis, K.; Panayiotou, C. Phase Compositions and Saturated Densities for the Binary Systems of Carbon Dioxide with Ethanol and Dichloromethane. *Fluid Phase Equilib.* **2004**, *224*, 89–96.
(18) Kneza, Z.; Skerget, M.; Ilic, L.; Lutge, C. Vapor-Liquid Equilibrium of Binary CO_2-Organic Solvent Systems Ethanol, tetra-Hydrofuran, ortho-Xylene, meta-Xylene, para-Xylene). *J. Supercrit. Fluids* **2008**, *43*, 383–389.
(19) Chen, H. I.; Chang, H. Y.; Huang, E. T. S.; Huang, T. C. A New Phase Behavior Apparatus for Supercritical Fluid Extraction Study. *Ind. Eng. Chem. Res.* **2000**, *39*, 4849–4852.
(20) Yeo, S. D.; Park, S. J.; Kim, J. W. S.; Kim, J. C. Critical Properties of Carbon Dioxide + Methanol, + Ethanol, + 1-Propanol, and + 1-Butanol. *J. Chem. Eng. Data* **2000**, *45*, 932–935.
(21) Yoon, J. H.; Lee, H. S.; Lee, H. High-Pressure Vapor−Liquid Equilibria for Carbon Dioxide + Methanol, Carbon Dioxide + Ethanol, and Carbon Dioxide + Methanol + Ethanol. *J. Chem. Eng. Data* **1993**, *38*, 53–55.
(22) Suzuki, K.; Sue, H. Isothermal Vapor-Liquid Equilibrium Data for Binary Systems at High Pressures: Carbon Dioxide−Methanol, Carbon Dioxide−Ethanol, Carbon Dioxide−*i*-Propanol, Methane−Ethanol, Methane−*i*-Propanol, Ethane−Ethanol, and Ethane−*i*-Propanol Systems. *J. Chem. Eng. Data* **1990**, *35*, 63–66.
(23) Joung, S. N.; Yoo, C. W.; Shin, H. Y.; Kim, S. Y.; Yoo, K. P.; Lee, C. S.; Huh, W. S. Measurements and Correlation of High-Pressure VLE of Binary CO_2-Alcohol Systems Methanol, Ethanol, 2-Methoxyethanol and 2-Ethoxyethanol). *Fluid Phase Equilib.* **2001**, *185*, 219–230.
(24) Galicia-Luna, L. A.; Ortega-Rodriguez, A. New Apparatus for the Fast Determination of High-Pressure Vapor-Liquid Equilibria of Mixtures and of Accurate Critical Pressures. *J. Chem. Eng. Data* **2000**, *45*, 265–271.
(25) Pfohl, O.; Pagel, A.; Brunner, G. Phase Equilibria in Systems Containing *o*-Cresol, p-Cresol, Carbon Dioxide, and Ethanol at 323.15−473.15 K and 10−35 MPa. *Fluid Phase Equilib.* **1999**, *157*, 53–79.
(26) Jennings, D. W.; Lee, R. J.; Teja, A. S. Vapor−Liquid Equilibria in the Carbon Dioxide + Ethanol and Carbon Dioxide + l-Butanol Systems. *J. Chem. Eng. Data* **1991**, *36*, 303–307.
(27) Kordikowski, A.; Schenk, A. P.; Van Nielen, R. M.; Peters, C. J. Volume Expansions and Vapor-Liquid Equilibria of Binary Mixtures of a Variety of Polar Solvents and Certain Near-Critical Solvents. *J. Supercrit. Fluids* **1995**, *8*, 205–216.
(28) Reaves, J. T.; Griffith, A. T.; Roberts, C. B. Critical Properties of Dilute Carbon Dioxide + Entrainer and Ethane + Entrainer Mixtures. *J. Chem. Eng. Data* **1998**, *43*, 683–683.
(29) Bamberger, A.; Maurer, G. High-Pressure Vapour + Liquid) Equilibria in Carbon Dioxide + Acetone or 2-Propanol) at Temperatures from 293 to 333 K. *J. Chem. Thermodyn.* **2000**, *32*, 685–700.
(30) Katayama, T.; Ohgaki, K.; Maekawa, G.; Goto, M.; Nagano, T. Isothermal Vapor-Liquid Equilibria of Acetone-Carbon Dioxide and Methanol-Carbon Dioxide Systems at High Pressures. *J. Chem. Eng. Jpn.* **1975**, *8*, 89–92.
(31) Adrian, T.; Maurer, G. Solubility of Carbon Dioxide in Acetone and Propionic Acid at Temperatures between 298 and 333 K. *J. Chem. Eng. Data* **1997**, *42*, 668–672.
(32) Kato, M.; Aizawa, K.; Kanahira, T.; Ozawa, T. A New Experimental Method of Vapor-Liquid Equilibria at High Pressures. *J. Chem. Eng. Jpn.* **1991**, *24*, 767–771.
(33) Soave-Redlich-Kwong, G. Equilibrium Constants from a Modified Redlich-Kwong Equation of State. *Chem. Eng. Sci.* **1972**, *27*, 1197–1203.
(34) Peng, D. Y.; Robinson, D. B. A New Two-Constant Equation of State. *Ind. Eng. Chem. Fundam.* **1976**, *15*, 59–64.
(35) Patel, N. C.; Teja, A. S. A New Cubic Equation of State for Fluids and Fluid Mixtures. *Chem. Eng. Sci.* **1982**, *37*, 463–473.
(36) Reid, R. C.; Prausnitz, J. M.; Poling, B. E. *The Properties of Gases and Liquids*, 4th ed.; McGraw-Hill: New York, 1984.
(37) Chiu, H. Y.; Jung, R. F.; Lee, M. J.; Lin, H. M. Vapor-Liquid Phase Equilibrium Behavior of Mixtures Containing Supercritical Carbon Dioxide near Critical Region. *J. Supercrit. Fluids* **2008**, *44*, 273–278.
(38) Isothermal Properties for Carbon Dioxide, NIST Chemistry WebBook, NIST Standard Reference Database No. 69-March 2003 Release, National Institute of Standard and Technology: USA, 2003 (http://webbook.nist.gov/chemistry/).
(39) Pfohl, O.; Petkov, S.; Brunner, G. *PE 2000- A Powerful Tool to Correlate Phase Equilibria*; Herbet Utz Verlag, Wissenschaft, Munchen: Germany, 2000.

Received for review May 23, 2008. Accepted July 24, 2008. The authors gratefully acknowledge the financial support from the National Science Council, Taiwan, through Grant No. NSC95-2214-E-011-154-MY3.

JE800371A